Small-Signal Analysis of Performance Characterization of Chaotic Masking Decoding in Injected Semiconductor Lasers

YAN Sen-Lin(颜森林)[1,2*]

[1]*Department of Physics, Nanjing Xiaozhuang College, Nanjing 210017*
[2]*School of Communication and Electronic Engineering, Jiangxi Science and Technology Normal University, Nanchang 330013*

(Received 4 June 2005)

Performance characterization of chaotic masking encoding and decoding is studied in synchronization injected semiconductor lasers under condition of injected-feedback. The modulation response function of chaotic masking encoding and its response factor are theoretically deduced and analysed by small-signal analysis. It is numerically demonstrated that there are peak values between 1.52 GHz and 3.18 GHz when the injection coefficient is between 0.2 and 0.8. The chaotic synchronization error equation is theoretically deduced and its root is given by small-signal analysis under condition of chaotic masking encoding. The chaotic decoding formula is also theoretically demonstrated. There are the least dale values of synchronization errors between the modulation frequencies of 0.79 GHz and 1.91 GHz when the injection coefficient is between 0.1 and 0.8 in numerical simulation. The numerical result is well consistent with the theoretical demonstration.

PACS: 05. 45. Vx, 05. 45. Pq

Chaotic optical communication is a promising technique to improve security in communication networks.[1−3] Secure optical communications based on a chaotic laser carrier have high-performance potential applications.[1,4,5] An all-optical chaotic approach would be attractive in high-speed and long-haul secure communications because all-optical systems have large bandwidth and low attenuation. Many semiconductor laser systems have been proposed for chaotic optical secure communications.[6−10] The techniques for using chaotic laser can be classified into three types: chaotic modulation, chaotic shift keying and chaotic masking.[6−10] In chaotic masking, a chaotic waveform is used for concealing a message. Due to the random nature and complexity of the chaotic waveform, such chaotic communication systems can be very difficult for encoding to attack. Therefore, it is an important issue to investigate message encoding and decoding performance characterization.

In this Letter, we analyse the performance characterization of chaotic masking encoding and decoding in injected semiconductor lasers[11] by a small-signal analysis method. We demonstrate theoretically and numerically the chaotic masking modulation response function, its response factor, synchronous error and decoding formula.

A message can be recovered from a transmission signal by subtracting the regenerated chaos from the received signal based on synchronization between the transmitter laser and the receiver laser in chaotic masking laser communication.[5−10] Figure 1 illustrates the synchronization model block based on injection semiconductor lasers with optical injection-feedback. The transmitter consists of master (M) laser, slave (S) laser diode (LD) and the receiver also consists of identical M-LD and S-LD. The M-LD output $E_m \exp[-j\omega_m t]$ injecting into S-LD, S-LD output $E(t)\exp\{-j[\omega_m t+\phi(t)]\}$ can become a chaotic state.[10,11] Synchronization can be realized by optical feedback in the receiver S-LD. We can use the Lang–Kobayashi equations to describe the dynamics of S-LDs due to M-LDs light injection,[1,6,10−13]

$$\begin{aligned}
\frac{dE_{t,r}}{dt} &= \frac{1}{2}(G_{t,r}-\gamma_p)E_{t,r}+\frac{k}{\tau_L}E_m\cos(-\phi_{t,r}) \\
&\quad + n_r\frac{f}{\tau_L}[E_t\cos(\phi_t-\phi_r)-E_r], \\
\frac{d\phi_{t,r}}{dt} &= \frac{1}{2}\beta_c(G_{t,r}-\gamma_p)+\frac{k}{\tau_L}\frac{E_m}{E_{t,r}}\sin(-\phi_{t,r}) \\
&\quad - \Delta\omega_m + n_r\frac{f}{\tau_L}\frac{E_t}{E_r}\sin(\phi_t-\phi_r), \\
\frac{dN_{t,r}}{dt} &= \frac{I}{q}-\gamma_{et,r}N_{t,r}-G_{t,r}V_pE_{t,r}^2, \qquad (1)
\end{aligned}$$

where k is the injection coefficient, both the receiver and feedback coefficients are denoted by f; the subscripts t and r indicate the transmitter and receiver $n_r=0$ for the transmitter and $n_r=1$ for the receiver; E and ϕ are the electrical amplitude and phase, N is the carrier number. The nonlinear mode gain is $G=(\Gamma v_g a/V)(N-N_{th})/\sqrt{1+E^2/E_s^2}$, where v_g is the group velocity of photon in the cavity, a is the gain constant, $\Gamma=V/V_p$ is the mode confinement factor, V is the active volume, V_p is the volume of the optical mode, E_s is the optical field amplitude in the photon saturation. $N_{th}=n_{th}V$ is the carrier number at transparency with density n_{th}. Here $\gamma_p=v_g(\alpha_m+\alpha_{int})$ is the photon loss rate, α_m is the cavity loss, α_{int} is the internal loss rate; $\Delta\omega_m=\omega_m-\omega_{th}$ is the stationary angular frequency detuning between the M-LD and S-LD; $\tau_L=2n_gL/c$ is the round-trip time in

* Email: yansenlinbsh@sina.com or senlinyan@163.com
©2005 Chinese Physical Society and IOP Publishing Ltd

the cavity length L; c is the light velocity in vacuum; $n_g = c/v_g$ is the group refractive index; I is the S-LD drive current; q is the unit charge; β_c is the linewidth enhancement factor; $\gamma_e = A_{nr} + B(N/V) + C(N/V)^2$ is the total carrier loss rate; A_{nr} is the nonradiative recombination rate, B is the radiative recombination coefficient taking into account the carrier loss induced by spontaneous emission; C is the Auger recombination coefficient. Under suitable parameters, theoretically, for time $t \to \infty$, if absolute value $|E_t - E_r| \to 0$, $|\phi_t - \phi_r| \to 0$, and $|N_t - N_r| \to 0$, and $|N_t - N_r| \to 0$, the receiver can be synchronized with the transmitter.

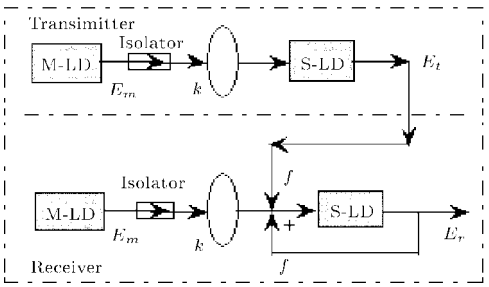

Fig. 1. Synchronization model block.

Let a message signal hide in a chaotic wave; then they are simultaneously transmitted into the optical channel, so that it is very difficult to detect the message if one does not know the system parameters.[5–10]

It is a necessary condition of chaotic secure communications that there are identical parameters between transmitter and receiver. Thus their stationary states would be the same in Eq. (1). In a stationary state, we ensure $E_{t0} = E_{r0} = E_0$, $\phi_{t0} = \phi_{r0} = \phi_0$, $N_{t0} = N_{r0} = N_0$. Due to small signal modulation in chaotic masking communications for better secrecy, the received signals are $E_{tm} = E_t(t) + s(t)$ and $|s| \ll E_t$, so small-signal analysis would be used to study chaotic masking encoding. The amplitude, phase, and carrier number are replaced by their static values added with their small variations. A small deviation relative to the static operating point is assumed as $\delta E_r, \delta\phi_r$ and δN_r. For the system (1), the injection intensity will have a main effect on synchronization and demodulation. We first analyse the effect of injection intensity on the receiver. We have $\delta\phi_t - \delta\phi_r \approx \delta(\phi_t - \phi_r) = 0$ and $\delta E_t - \delta E_r \approx \delta(E_t - E_r) = 0$ after synchronization. The response equation about the chaotic masking modulation of the receiver is yielded to the first-order approximation as follows:

$$\frac{d}{dt}\begin{pmatrix}\delta E_r\\ \delta\phi_r\\ \delta N_r\end{pmatrix} = \begin{pmatrix}A_{11} & A_{12} & A_{13}\\ A_{21} & A_{22} & A_{23}\\ A_{31} & A_{32} & A_{33}\end{pmatrix}\begin{pmatrix}\delta E_r\\ \delta\phi_r\\ \delta N_r\end{pmatrix} + \begin{pmatrix}1\\0\\0\end{pmatrix}\delta S \tag{2}$$

where

$$S(t) = k_r s(t), \quad k_r = f/\tau_L,$$
$$A_{11} = \frac{1}{2}(G_0 - \gamma + E_0 G_E),$$
$$A_{21} = \frac{1}{2}\beta_c G_E - \frac{k}{\tau_L}\frac{E_m}{E_0^2}\sin(-\phi_0),$$
$$A_{12} = \frac{k}{\tau_L}E_m \sin(-\phi_0),$$
$$A_{22} = -\frac{k}{\tau_L}\frac{E_m}{E_0}\cos(-\phi_0),$$
$$A_{13} = \frac{1}{2}E_0 G_N, \quad A_{23} = \frac{1}{2}\beta_c G_N,$$
$$A_{31} = -2G_0 E_0 V_p - E_0^2 V_p G_E,$$
$$G_N = \frac{\partial G}{\partial N}\Big|_{N=N_0,E=E_0}, \quad A_{32} = 0,$$
$$G_E = \frac{\partial G}{\partial E}\Big|_{N=N_0,E=E_0},$$
$$A_{33} = -\gamma_{e0} - N_0\gamma_{eN} - E_0^2 V_p G_N,$$
$$\gamma_{eN} = \frac{\partial \gamma_e}{\partial N}\Big|_{N=N_0}.$$

A small signal modulation response function is defined by

$$G(\omega) = \frac{\delta E_r(\omega)}{\delta E_{tm}(\omega)}. \tag{3}$$

The response factor is also defined by

$$g(\omega) = \frac{\delta E_r(\omega)}{\delta s(\omega)} = \frac{G(\omega)}{G(\omega) - 1}, \tag{4}$$

$$G(\omega) = \frac{1}{1 + 1/g(\omega)}. \tag{5}$$

From Eq. (2), we obtain

$$G(\omega) = \left(j\omega A_{33}k_r - \omega^2 k_r + A_{11}A_{22}k_r\right) \cdot \left[-j\omega^3 - \omega^2(b_1 + k_r) - j\omega(b_2 - A_{33}k_r) + (b_3 + A_{22}A_{33}k_r)\right]^{-1}, \tag{6}$$

$$g(\omega) = \frac{j\omega A_{33}k_r - \omega^2 k_r + A_{33}A_{22}k_r}{-j\omega^3 - \omega^2 b_1 - j\omega b_2 + b_3}, \tag{7}$$

where

$$b_1 = -(A_{11} + A_{22} + A_{33}),$$
$$b_2 = (A_{31}A_{13} - A_{11}A_{22} + A_{12}A_{21} - A_{33}A_{11} - A_{33}A_{22}),$$
$$b_3 = -(A_{31}A_{12}A_{23} - A_{31}A_{13}A_{22} + A_{33}A_{11}A_{22} - A_{33}A_{12}A_{21}).$$

The amplitude of the response function is

$$|G(\omega)| = \left[\omega^2 A_{33}^2 k_r^2 + (\omega^2 k_r - A_{22}A_{33}k_r)^2\right]^{1/2} \cdot \left\{[\omega^3 + \omega(b_2 - A_{33}k_r)]^2 + [\omega^2(b_1 + k_r) + (b_3 + A_{22}A_{33}k_r)]^2\right\}^{-1/2}, \tag{8}$$

and the amplitude of the response factor is

$$|g(\omega)| = \sqrt{\frac{\omega^2 A_{33}^2 k_r^2 + (\omega^2 k_r - A_{22}A_{33}k_r)^2}{(\omega^3 + \omega b_2)^2 + (\omega^2 b_1 - b_3)^2}}. \tag{9}$$

From Eq. (9), the amplitude of the response factor increases with the increasing injection coefficients. Using the parameters listed in Table 1, we can obtain the numerical results as shown in Fig. 2. There are the peak values presenting in the response function.

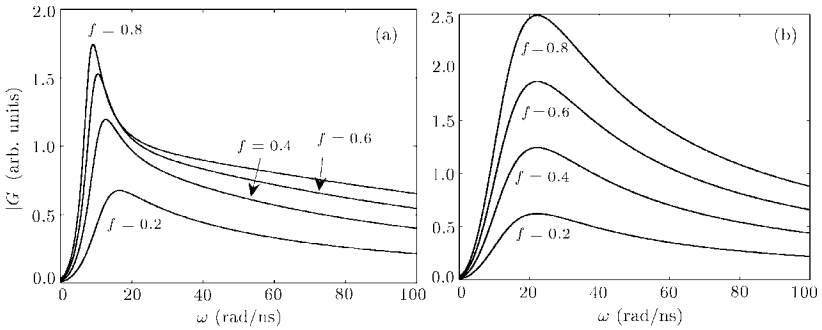

Fig. 2. Response function (a) and response factor (b) under small signal modulation.

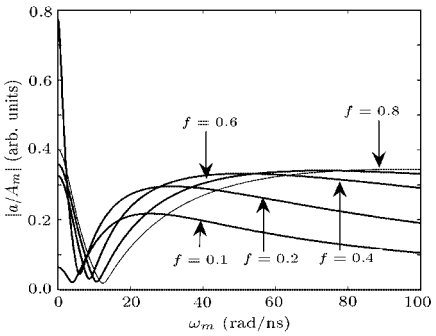

Fig. 3. Synchronization errors versus modulation frequency for different feedback coefficient f.

For example, there is a peak value at frequency of 3.18 GHz for $f = 0.2$ in Fig. 2(a). The largest modulation response shows at frequency of 3.18 GHz for $f = 0.2$, but the peak position moves to lower frequency with the increasing modulation intensity, namely, from 3.18 GHz to 1.52 GHz. Figure 2(b) illustrates that there are the largest modulation response factors at 3.18 GHz, which is approximately equal to the chaotic wave frequency. Figure 2 also illustrates that the response function and the response factor increases with the increasing injection coefficient, and the modulation bandwidth would reach about 15 GHz. However, the response amplitude gradually decreases at higher frequencies, which also illustrates that the effect of modulation response trails off at high frequency, and the response amplitude obviously decreases at lower frequencies.

Table 1. LD parameters.

Symbol	Value	Symbol	Value
L (μm)	350	B (cm^3/s)	1.2×10^{-10}
W (μm)	2	C (cm^6/s)	3.5×10^{-29}
d (μm)	0.15	E_s (m$^{-3/2}$)	1.6619×10^{11}
Γ (μm)	0.29	a (cm^2)	2.3×10^{-16}
n_g	3.8	β_c	6
α_m (cm^{-1})	29	$\Delta\omega$ (rad/s)	6
α_{int} (cm^{-1})	20	I (mA)	25
n_{th} (cm^{-3})	1.2×10^{18}	E_m (m$^{-3/2}$)	$0.126\,E_s$
A_{nr} (s^{-1})	1.0×10^8	k	0.033

Due to small signal modulation, Eq. (1) yields a synchronous error equation to the first-order approximation as follows:

$$\frac{d}{dt}\begin{pmatrix}\delta(E_t-E_r)\\ \delta(\phi_t-\phi_r)\\ \delta(N_t-N_r)\end{pmatrix} = \begin{pmatrix}B_{11} & A_{12} & A_{13}\\ A_{21} & B_{22} & A_{23}\\ A_{31} & A_{32} & A_{33}\end{pmatrix} \cdot \begin{pmatrix}\delta(E_t-E_r)\\ \delta(\phi_t-\phi_r)\\ \delta(N_t-N_r)\end{pmatrix} - \begin{pmatrix}k_r\\ 0\\ 0\end{pmatrix} s(t), \quad (10)$$

where $B_{11} = A_{11} - k_r$ and $B_{22} = A_{22} - k_r$. The real parts of all the eigenvalues are negative in Eq. (4) so that synchronization is achieved between the transmitter and the receiver when $0.05 < f < 1$ in numerical calculations. The instantaneous error of chaotic synchronization is written as $E_t - E_r \approx \delta E_t - \delta E_r = \delta(E_t - E_r) = \delta e(t)$. A synchronous error equation to the first-order approximation is obtained by

$$\frac{d^3}{dt^3}\delta e + B_1\frac{d^2}{dt^2}\delta e + B_2\frac{d}{dt}\delta e + B_3\delta e = A_{33}B_{22}S(t) + \frac{d^2}{dt^2}S(t) - A_{33}\frac{d}{dt}S(t), \quad (11)$$

where

$$\begin{aligned} B_1 &= -(B_{11} + B_{22} + A_{33}),\\ B_2 &= -(A_{31}A_{13} - B_{11}B_{22} + A_{12}A_{21} - A_{33}B_{11} - A_{33}B_{22}),\\ B_3 &= -(A_{31}A_{12}A_{23} - A_{31}A_{13}B_{22} + A_{33}B_{11}B_{22} - A_{33}A_{12}A_{21}). \end{aligned}$$

If the modulation signal is written as a complex function, we can obtain $s = A_m \exp(-j\omega_m t)]$ with $\omega_m = 2\pi f_m$, where A_m is the modulation depth and f_m is the modulation frequency. We assume that the instantaneous error function is similar to the modulation signal expression because the synchronization error is from the modulation signal perturbation after synchronization. Supposing $\delta e(t) = a\exp(-j\omega_m t)$, one obtains the following complex instantaneous error of chaotic synchronization:

$$a = \frac{(j\omega_m A_{33} - \omega_m^2 + A_{33}B_{22})k_r A_m}{-j\omega_m^3 - \omega_m^2 B_1 - j\omega_m B_2 + B_3} \quad (12)$$

or

$$|a| = \sqrt{\frac{\omega_m^2 A_{33}^2 k_r^2 + (\omega_m^2 - A_{33}B_{22}^2)^2 k_r^2}{(\omega_m^3 + \omega_m B_2)^2 + (\omega_m^2 B_1 - B_3)^2}}\, A_m = \gamma A_m, \quad (13)$$

where

$$\gamma = \sqrt{\frac{\omega_m^2 A_{33}^2 k_r^2 + (\omega_m^2 - A_{33}B_{22}^2)^2 k_r^2}{(\omega_m^3 + \omega_m B_2)^2 + (\omega_m^2 B_1 - B_3)^2}}$$

and the phase

$$\varphi = \mathrm{tg}^{-1}\Big\{[(B_3 - \omega_m^2 B_1)(A_{33}B_{22} - \omega_m^2) - \omega_m^2 A_{33}(\omega_m^3 + \omega_m B_2)][\omega_m A_{33}(B_3 - \omega_m^2 B_1) + (A_{33}B_{22} - \omega_m^2)(\omega_m^3 + \omega_m B_2)]^{-1}\Big\}. \quad (14)$$

The instantaneous error is increased with the increasing modulation signal due to the error being from the modulation signal after synchronization. The numerical result is shown in Fig. 3. The dale strata of the least instantaneous error is at a frequency position of 5,rad/ns≈ 0.79 GHz for $f = 0.1$. The least dale strata is at a frequency of 6 rad/ns≈ 0.95 GHz for $f = 0.2$. Similarly, 9 rad/ns≈ 1.43 GHz for $f = 0.4$, 6 rad/ns≈ 0.95 GHz for $f = 0.6$, 11 rad/ns≈ 1.75 GHz for $f = 0.8$. The least instantaneous errors move to higher frequencies with the increasing injection coefficient.

The demodulated signal $s_d(t)$ is deduced from Eqs. (10)–(14),

$$\begin{aligned} s_d(t) &= E_t(t) + s(t) - E_r(t) \approx \delta e(t) + s(t) \\ &= a\exp[-j(\omega_m t - \varphi)] + A_m \exp(-j\omega_m t) \\ &= [\gamma \exp(-j\varphi) + 1] A_m \exp(-j\omega_m t). \end{aligned} \tag{15}$$

The quality of decoding and demodulated signal is related with both the synchronization error and its phase from Eq. (15). Thus the stationary phase must be considered for demodulation quality. Because of $|\gamma| < 1$, the encoding process may be practically achieved.

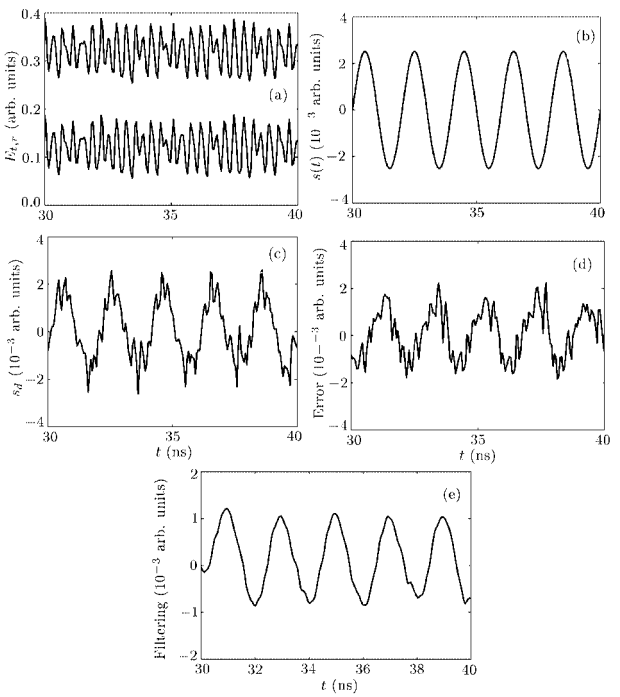

Fig. 4. Decoding after synchronization.

The chaotic masking encoding and demodulation are numerically simulated by taking $f = 0.5$. Figure 4(a) illustrates the synchronization between the transmitter and the receiver at a modulation frequency of 0.5 GHz and at amplitude of $2\%E_s$, where above is the receiver waveform which is over the paralleled 0.2 unit and below is the transmitted chaotic wave masking the message signal. Figure 4(b) shows the message signal and Fig. 4(c) shows the instantaneous synchronization error in the demodulation process that is similar to the message signal realized from Eqs. (11)–(14), whereas its variably would have a stationary phase error to the modulated signal, where $|a| = 8.8136 \times 10^{-4} \ll A_m = 4.52 \times 10^{-3}$, namely $|a/A_m| = 19.49\%$ or the rate of the signal to the error $|A_m/a| \approx 5.13$, so chaotic decoding, which is consistent with the theoretical demonstration and numerical calculation, can be practically achieved. Figure 4(d) shows the decoded signal, which is in good agreement with the modulated message signal in spite of synchronization error affecting decoding quality to a certain extent. Figure 4(e) shows a low-pass filter process, in which the filtered signal is in good agreement with the modulated message signal.

Channel noise influence should be considered on demodulation. Provided that the white noise is dominant and much higher than other noises and it is added on the transmitted signal, then the white noise and the transmitted signal should be simultaneously received by the receiver. Using the parameters taken in Fig. 4, for the white noise, we let the noise mean values be zero and the squared errors be $10\%A_m$, $30\%A_m$ and $50\%A_m$, respectively, which are very large. In this case, the demodulation can still be realized. However, the demodulation squared errors are about 21%, 41% and 144%, respectively, higher than the errors without any noise in the numerical analysis. The demodulation cannot be achieved with a higher than $50\%A_m$ noise. In order to improve the demodulation quality, a low-pass filter can be used to filter the received signal to eliminate the noise perturbation on the demodulation.

In summary, performance characterization of chaotic masking encoding and decoding has been studied by a small-signal analysis. The modulation response function and response factor are theoretically deduced and analysed. There are the peak values of the response function and the response factor in the numerical simulation. The chaotic synchronization error equation and the chaotic decoding formula are demodulated theoretically and numerically. It is very useful for chaotic encoding and decoding applications in secure communications.

References

[1] Colet P and Roy R 1994 *Opt. Lett.* **19** 2056
[2] Liu Z R and Mao J M 2003 *Chin. Phys. Lett.* **20** 206
[3] Qi H J et al 2003 *Chin. Phys. Lett.* **20** 622
[4] Feng J C and Qiu Y H 2004 *Chin. Phys. Lett.* **21** 250
[5] Lu H P et al 2004 *Chin. Phys. Lett.* **21** 1016
[6] Wu L and Zhu S Q 2003 *Chin. Phys.* **12** 300
[7] Hua C C and Guan X P 2004 *Chin. Phys. Lett.* **21** 1441
[8] Xu J F et al 2004 *Chin. Phys. Lett.* **21** 1445
[9] Chen S Y et al 2004 *Chin. Phys. Lett.* **21** 2128
[10] Ma K et al 2003 *Chin. Phys. Lett.* **20** 2118
[11] Yan S L, Chi Z Y and Chen W J 2004 *Sci. Chin.* F **47** 332
[12] Troger J and Nicati P A 1999 *IEEE J. Quantum Electron.* **35** 1713
[13] Atsushi U, Yun L and Perter D 2003 *IEEE J. Quantum Electron.* **39** 963